

A New Series of Isorecticular Copper-Based Metal-Organic Frameworks Containing Non-Linear Linkers with Different Group 14 Central Atoms

*Stephanie E. Wenzel, Michael Fischer, Frank Hoffmann, and Michael Fröba**

Institute of Inorganic and Applied Chemistry, Department of Chemistry, University of Hamburg,

Martin-Luther-King-Platz 6, D-20146 Hamburg, Germany

michael.froeba@chemie.uni-hamburg.de

*) Michael.Froeba@chemie.uni-hamburg.de, Tel: +49-40-42838-3137, Fax: +49-40-42838-6348

Supporting Information

- (1) EDX-analyses of **UHM-3-4**.
- (2) Magnified view of the P-XRD patterns of **UHM-2** and **UHM-4** in the region $20 - 35^\circ 2\theta$.
- (3) PXRD pattern of activated **UHM-2**, **UHM-4**, and **UHM-3-4**.
- (4) Thermal analyses of **UHM-2**, **UHM-4**, and **UHM-3-4**.
- (5) Isotherm series for determination of the isosteric heats of adsorption.
- (6) Illustration of the mode of interactions of the hydrogen molecule with the model linker systems.

(1) EDX-analyses of UHM-3-4.

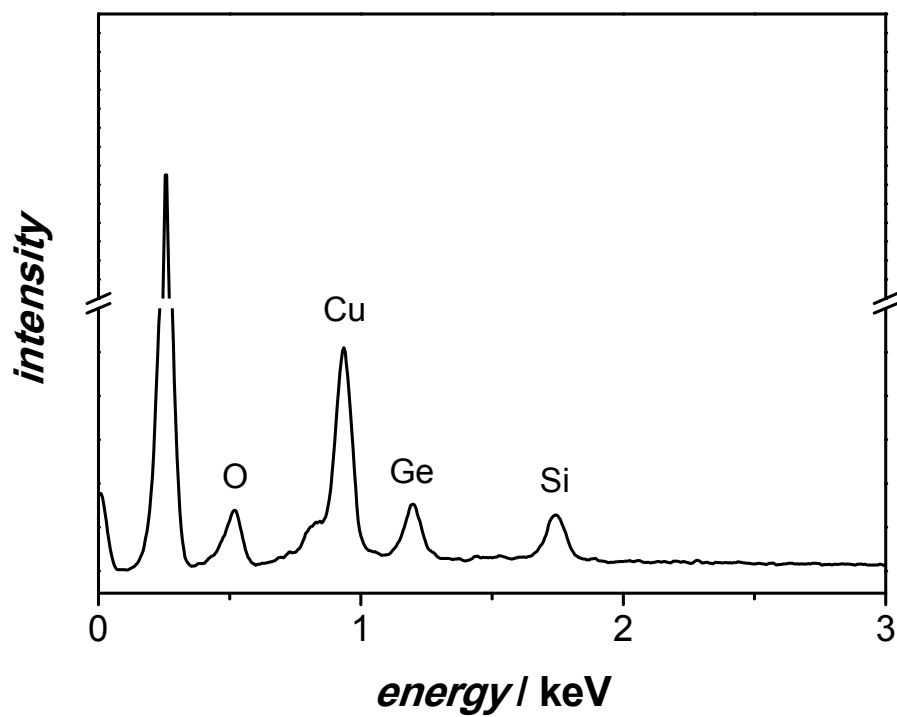


Figure S-1: EDX-Analyses of UHM-3(50)-4(50).

(2) Magnified view of the P-XRD patterns of UHM-2 and UHM-4 in the region 20 – 35 ° 2 θ .

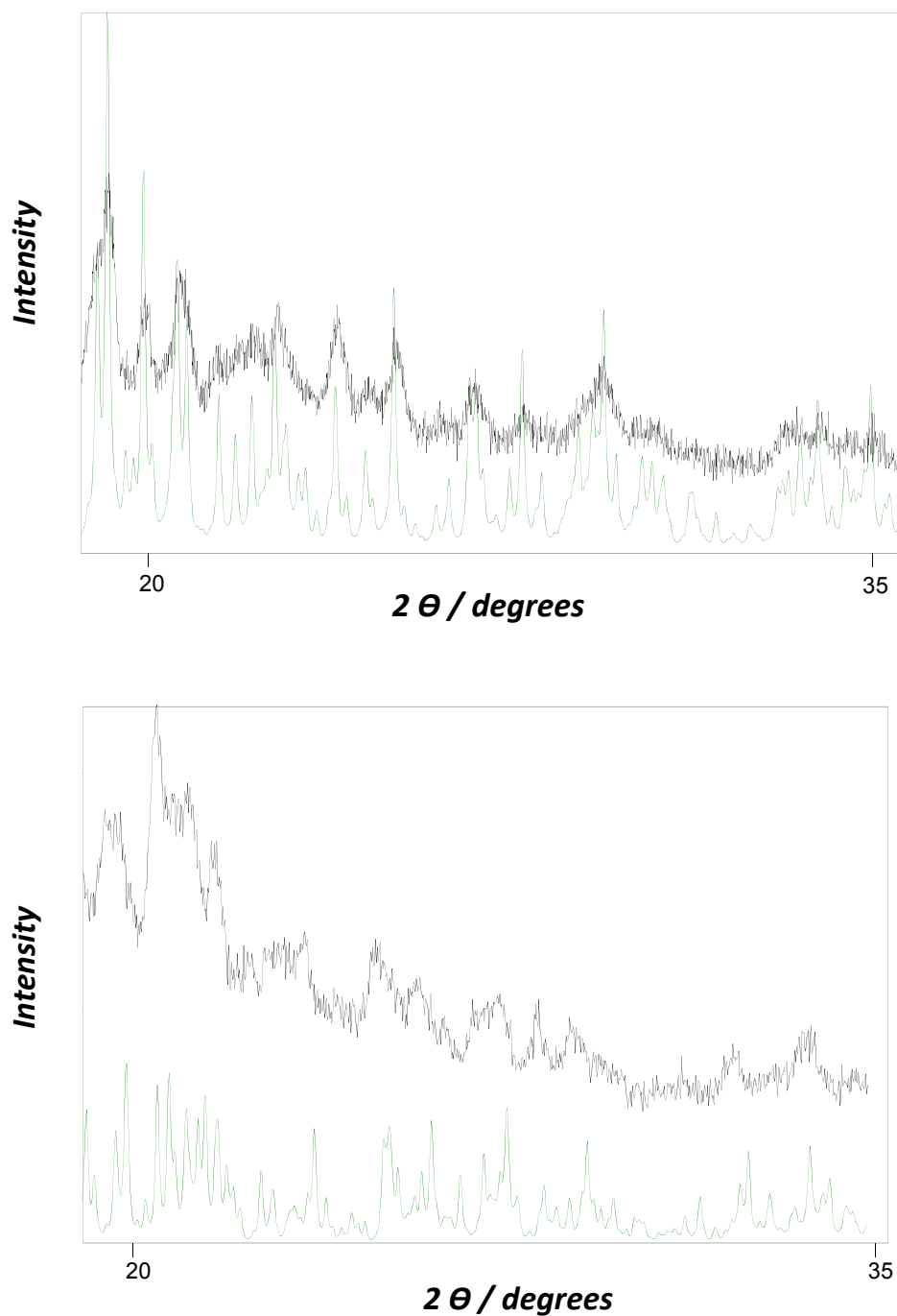


Figure S-2: Comparison of the experimental (black) and simulated (green) P-XRD patterns of **UHM-2** (top) and **UHM-4** (bottom).

(3) PXRD pattern of activated UHM-2, UHM-4, and UHM-3-4.

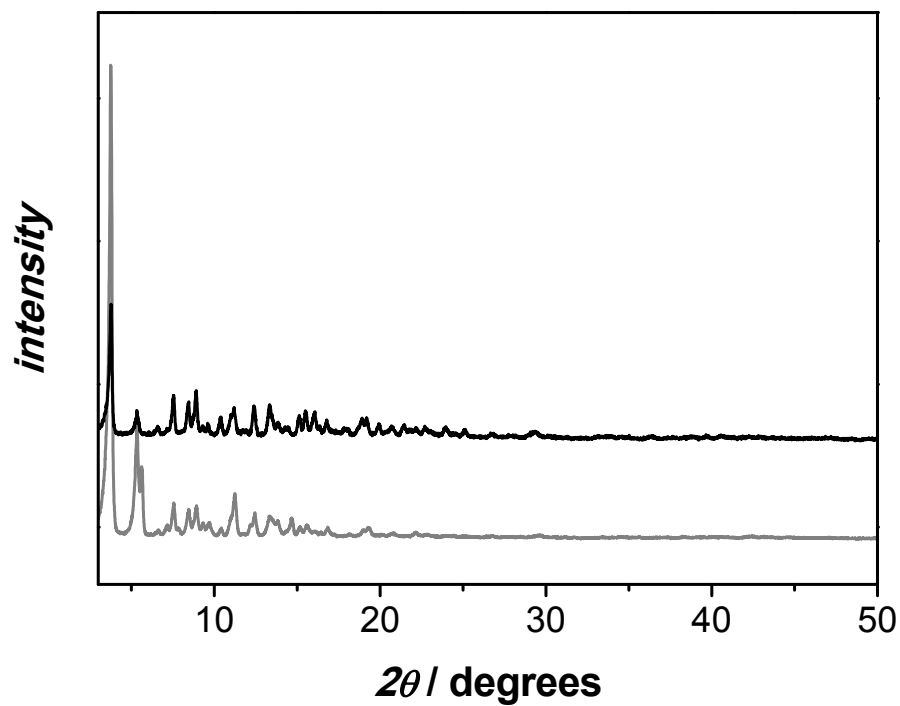


Figure S-3a: Powder X-Ray diffraction patterns of as synthesized **UHM-2** (black) and activated **UHM-2** (gray, 24 h, 170 °C).

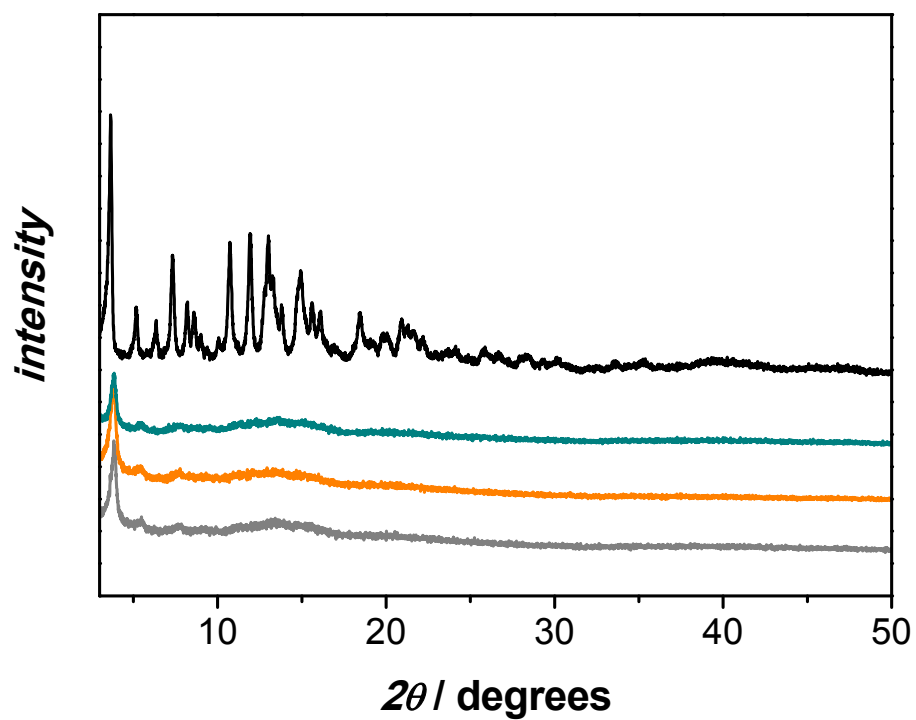


Figure S-3b: Powder X-Ray diffraction patterns of as synthesized UHM-4 (black) and activated UHM-4 (green, 24 h, 100 °C; orange, 24 h, 120 °C and gray, 24 h, 150 °C).

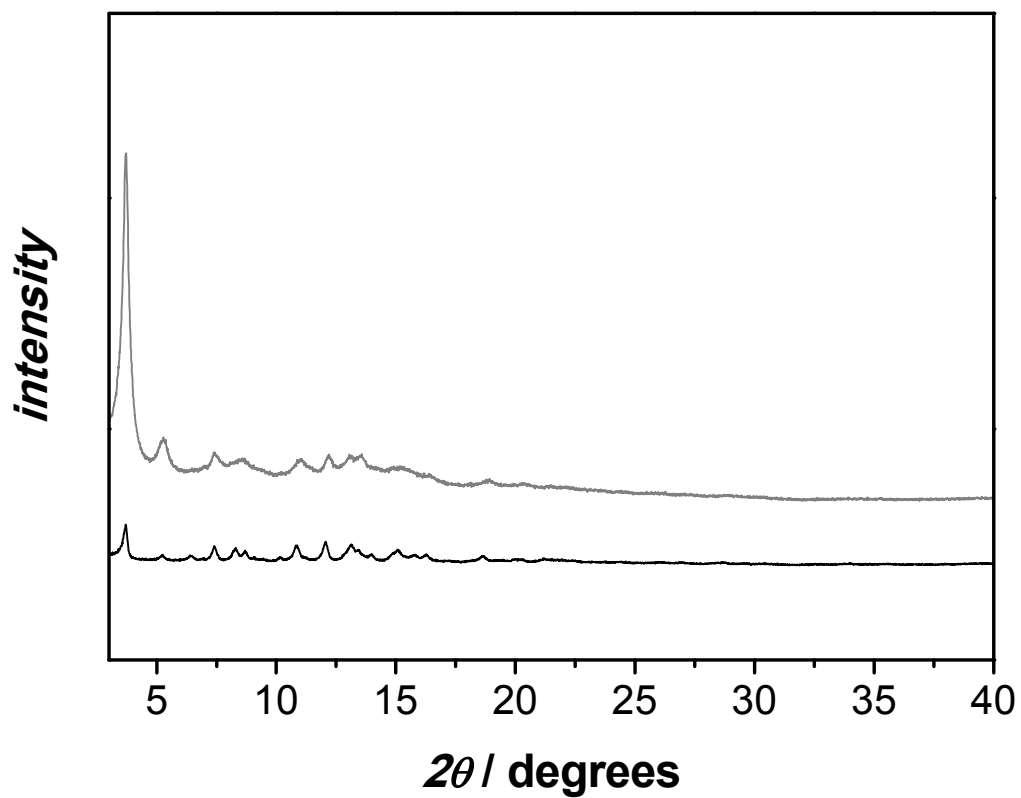


Figure S-3c: Powder X-Ray diffraction patterns of as synthesized (black) and activated UHM-3(50)-4(50) (gray, 24 h, 150 °C).

(4) Thermal analyses of UHM-2, UHM-4, and UHM-3-4.

Thermal Analyses.

To study the thermal stability of as synthesized UHM-2 and UHM-4 TG-MS and DTA were carried out (figure S-4a and S-4b).

The overall mass decrease of UHM-2 can be roughly divided into two parts. In a first step between 25 °C and 226 °C, the material shows a mass loss of 22 % due to the loss of DMSO corresponding to the detected mass $m/z = 63$, which is characteristic for the fragment ion CH_3SO^+ . At 226 °C the thermal decomposition of the network starts generating water and carbon dioxide (H_2O^+ , $m/z = 18$; CO_2^+ , $m/z = 44$). In this step up to 678 °C a weight loss of 49 % is observed. However, DMSO is still detected up to 337 °C indicating a delayed desolvation, which slightly overlaps with the thermal decomposition of the material.

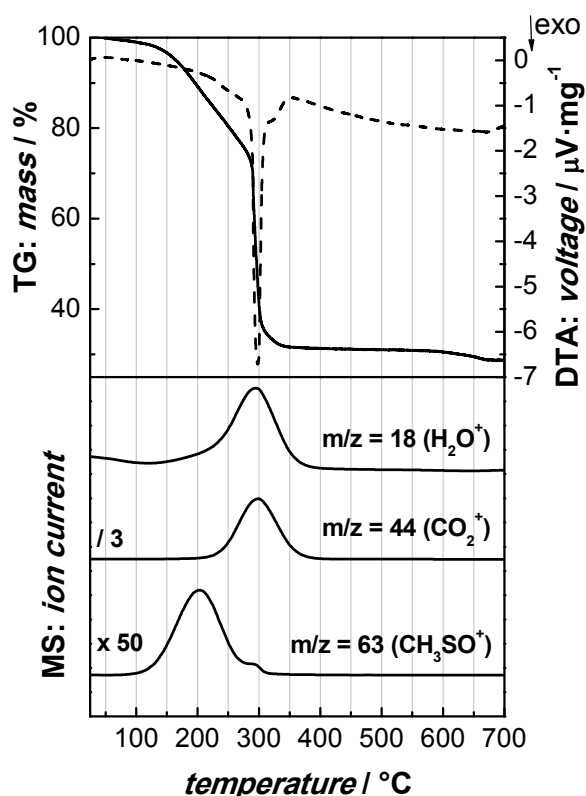


Figure S-4a: TG-MS and DTA of as synthesized UHM-2.

The mass loss of **UHM-4** can be roughly divided into three steps. The first weight decrease of 26 % up to 93 °C is caused by dehydration and accompanied by the detection of water (H_2O^+ , $m/z = 18$). In the second step between 93 °C and 223 °C with a weight loss of 22% predominantly DMA ($\text{C}_4\text{H}_9\text{NO}^+$, $m/z = 87$) is detected. The thermal decomposition of **UHM-4** starts at 223 °C (H_2O^+ , $m/z = 18$; CO_2^+ , $m/z = 44$) indicating that the material is less stable than **UHM-2** caused by the weak Ge-C-bond. Up to 608 °C a weight loss of 45 % is observed in this step. Analogue to **UHM-2** solvent loss overlaps slightly with thermal composition.

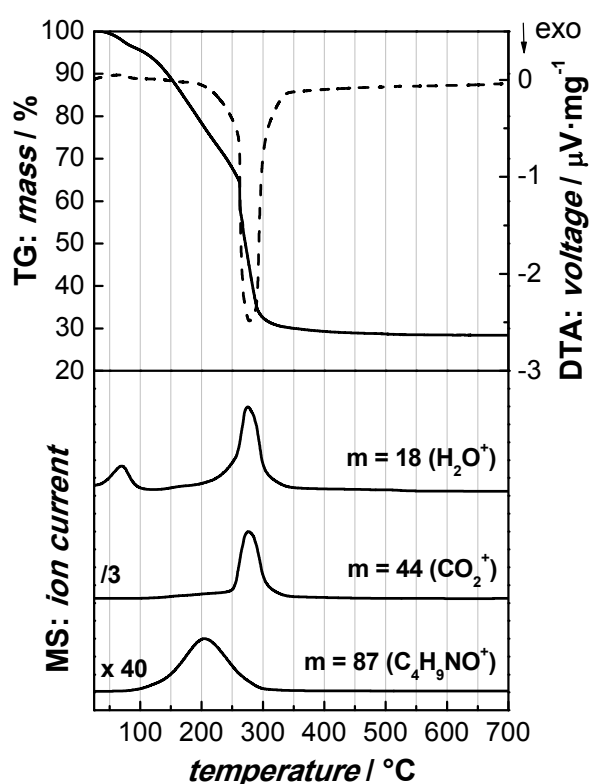


Figure S-4b: TG-MS and DTA of as synthesized **UHM-4**.

For **UHM-3(50)-4(50)** overall mass decrease occurs in three steps (Figure S-4c). First, up to 96 °C dehydration takes place, The corresponding weight loss of 1.2 % is accompanied by the detection of water (H_2O^+ , $m/z = 18$). Up to 224 °C a mass loss of 14.5 % is observed, which is predominantly caused by the loss of DMA ($\text{C}_4\text{H}_9\text{NO}^+$, $m/z = 87$). Thermal decomposition starts at 224 °C (similar to **UHM-4**) generating thereby water and carbon dioxide (H_2O^+ , $m/z = 18$; CO_2^+ , $m/z = 44$). At 523 °C the weight

loss of additional 46.7 % ends. During thermal decomposition of the mixed MOF DMA was also detected, which again proves a delayed desolvation.

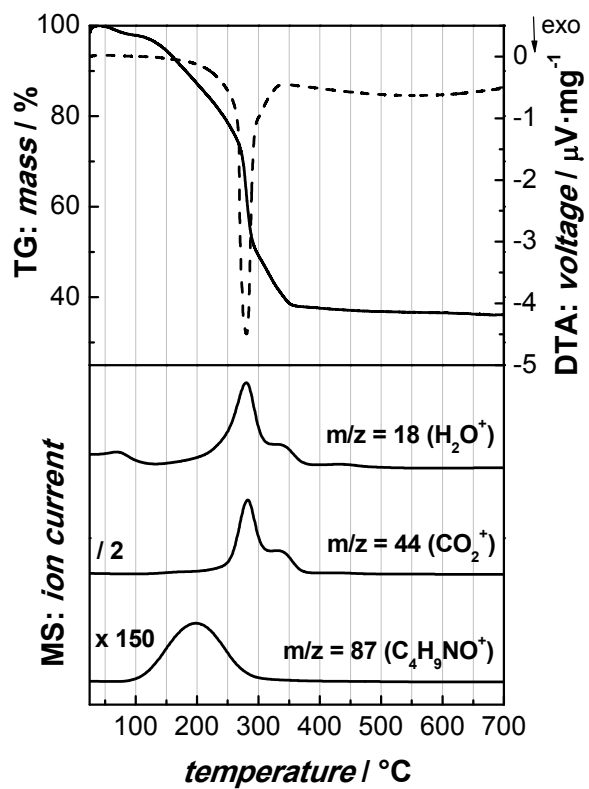


Figure S-4c: TG-MS and DTA of as synthesized UHM-3(50)-4(50).

(5) Isotherms for determination of the isosteric heats of adsorption.

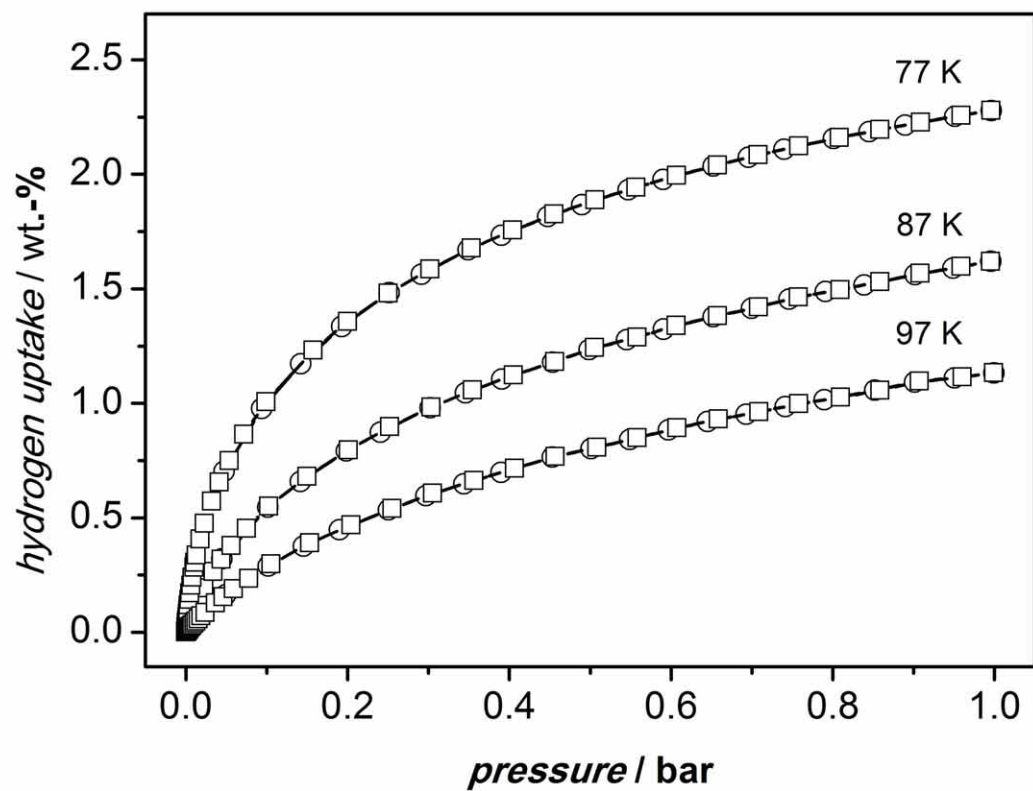


Figure S-5a: Hydrogen physisorption isotherms (\square , adsorption; \circ , desorption) of activated **UHM-2** at 77 K, 87 K and 97 K.

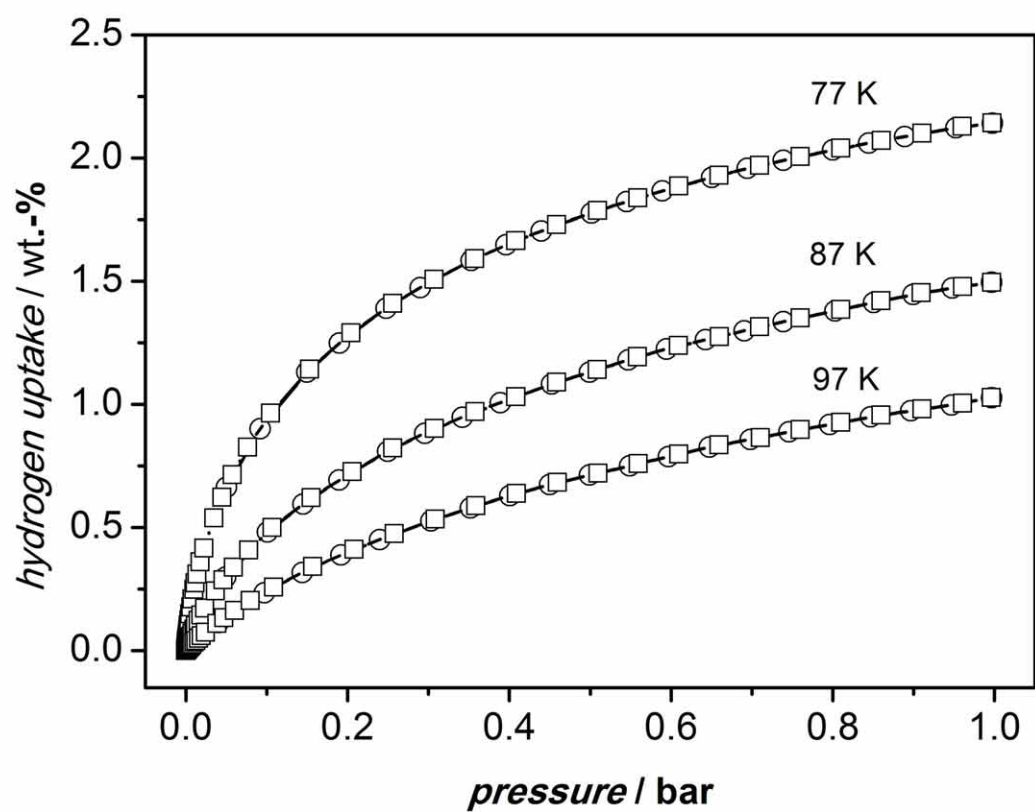


Figure S-5b: Hydrogen physisorption isotherms (\square , adsorption; \circ , desorption) of activated **UHM-3** at 77 K, 87 K and 97 K.

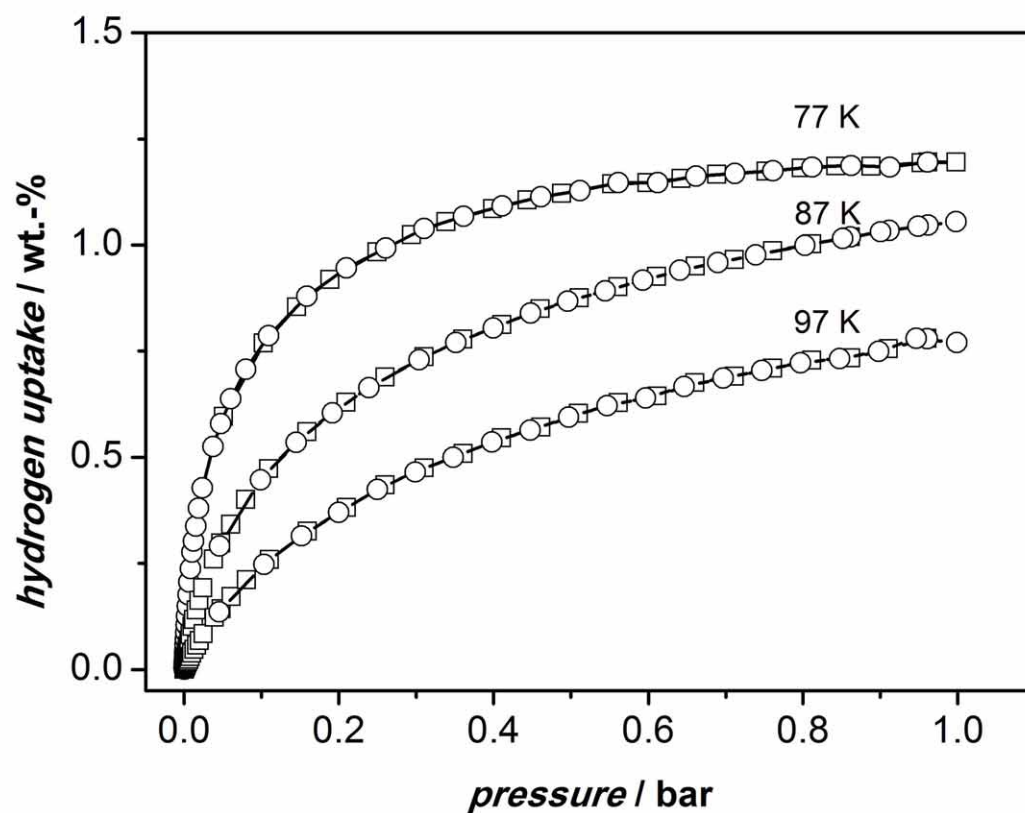


Figure S-5c: Hydrogen physisorption isotherms (\square , adsorption; \circ , desorption) of activated **UHM-4** at 77 K, 87 K and 97 K.

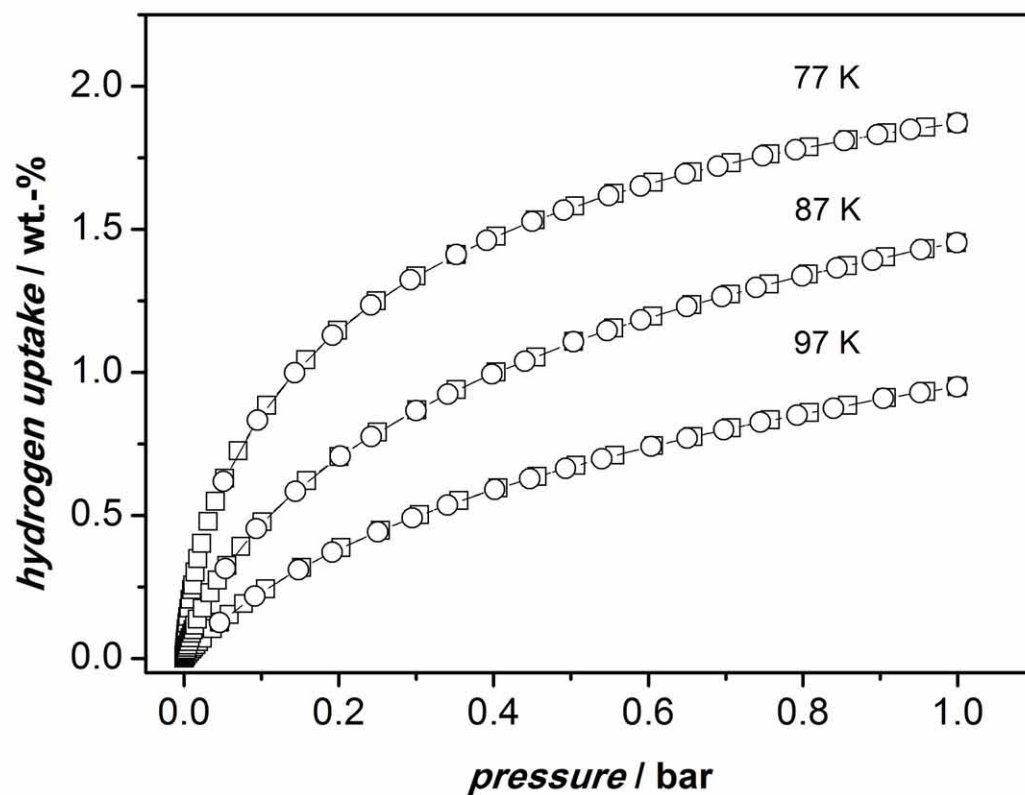


Figure S-5d: Hydrogen physisorption isotherms (\square , adsorption; \circ , desorption) of activated UHM-3(50)-4(50) at 77 K, 87 K and 97 K.

(6) Illustration of the mode of interactions of the hydrogen molecule with the model linker systems.

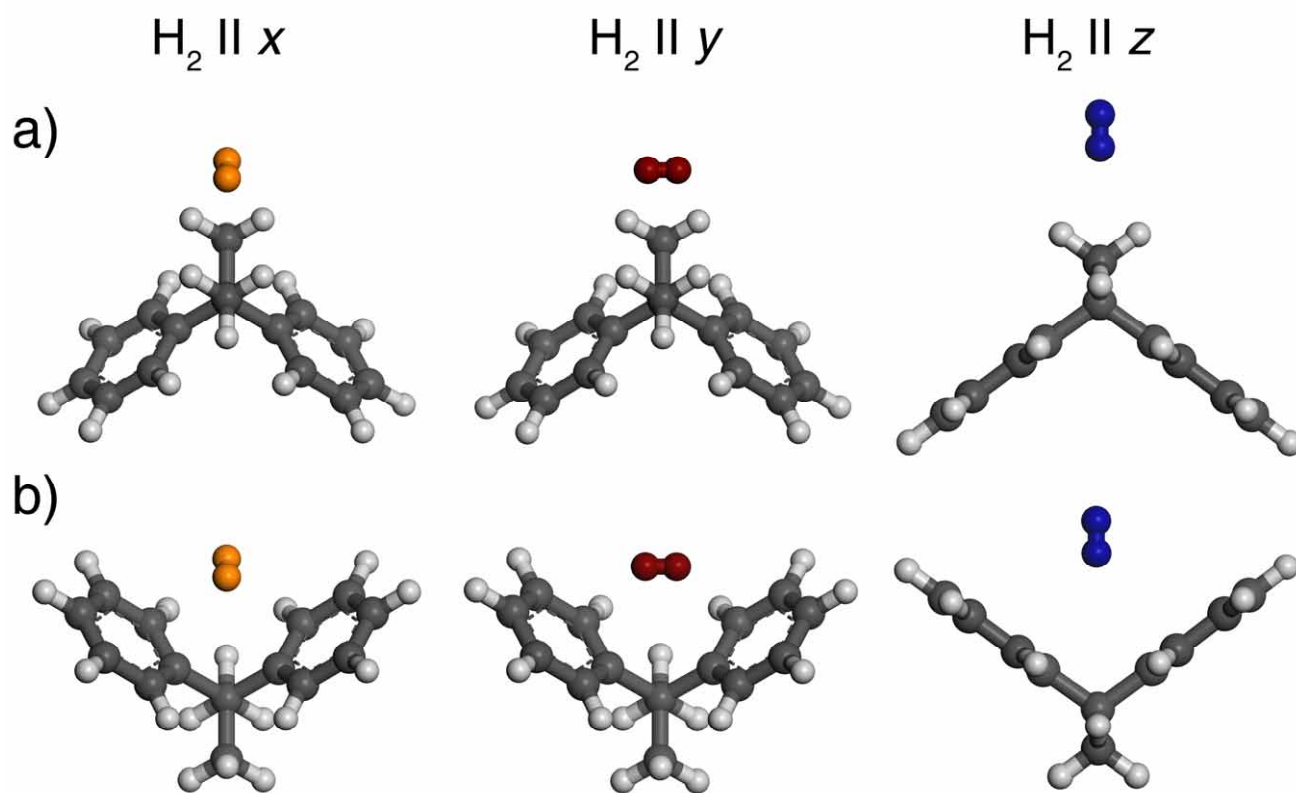


Figure S-6: Illustration of the approach of the hydrogen molecule towards the central unit of the model linker systems, along the z -axis from the side of the methyl groups (a, b) and along the z -axis from the side of the phenyl groups (c).